Journal of Research and Applications in Mechanical Engineering
ISSN: 2229-2152 (Print); 2697-424x (Online)
(2021) Vol. 9, No. 2, Paper No. JRAME-21-9-013
[DOI: 10.14456/jrame.2021.13]

Research Article

IMPROVEMENT OF ESTIMATION METHOD FOR BATTERY CELL HEAT GENERATION

J. Kulranut[1]
N. Depaiwa [1]
T. Yenwichai [2]
W. Intano [2]
M. Masomtob [2,*]
[1] *School of Engineering, King Mongkut's Institute of Technology Ladkrabang, Chalongkrung Road, Ladkrabang, Bangkok, 10520, Thailand*
[2] *National Energy Technology Center (ENTEC), National Science and Technology Development Agency (NSTDA), 114 Thailand Science Park, Pathumthani, 12120, Thailand*

Received 21 December 2020
Revised 17 February 2021
Accepted 18 February 2021

ABSTRACT:
This work represents a new experimental method to precisely estimate the heat generation of the battery cell by reducing heat losses to the ambient. The temperature ambient in the chamber is controlled to be close to the battery cell temperature as much as possible in order to reduce the heat loss from the battery to the ambient. The battery is covered by an insulator, and the heat loss due to the heat conduction at the electric connectors is also considered. Therefore, the heat generation term is absorbed by the heat capacity term; in other words, the heat generation of the battery cell can be calculated via the rising temperature of the heat capacity term and the heat loss of the connectors. Consequently, this new method can obtain the precision of the estimated heat generation that can be used to design an appropriate battery thermal management system for the battery pack.

Keywords: *Battery cell, Battery thermal management system, Heat generation*

1. INTRODUCTION

Nowadays, lithium-ion or Li-ion batteries are widely used as a choice of power sources for small handheld electronic devices, hybrid electric vehicles (HEVs), and electrical vehicles (EVs) because of its high specific energy, low self-discharge rate, no memory effect, and low self-discharge [1]. The temperature increase during the high-power extraction in HEV and EV applications is the main concern as the occurrence can cause battery degradation and the thermal runaway .It is thus vital to maintain the temperature below a certain limit for the prevention of the battery failure due to the thermal runaway .The temperature increase can degrade the battery performance significantly . Therefore, design tools are required to predict the thermal behavior of the batteries so that the designed products could be manufactured with the appropriate cooling systems.

There are many previous studies on thermal modeling in order to calculate the heat generation in a Li-ion battery cells. Y. Abdul-Quadir et al.[2] present the formula for total heat that generated in a Li-ion battery cells, the formula composes of two terms which are the overpotential heat and the entropic heat. The overpotential heat, can be measured via the overpotential resistance by four different methods. And the entropic heat can be measured by the rate of self-discharge relative to the temperatures. Ying Bai et al. [3] propose the method for calculating the heat generation rate by calculated the entropic coefficients and internal resistance of battery in adiabatic environment. Wang et al. [4] present a method for measuring the amount of heat and simulate the heat release during the charging and discharging

* Corresponding author: M. Masomtob
E-mail address: manop.mas@entec.or.th

by the thermal condition monitoring system to obtain the temperature of a lithium-ion battery under the electrical heating conditions. Chunjing Lin et al. [5] present the method for the evaluation of the heat generation by using an extended volume accelerating rate calorimetry. Peammawat et al. [6] show the method to examine heat generation in a battery resulting from entropy change. An entropy change in a battery cell is measured by a trial and error process to fit the temperature behavior curve. Nicolas Damay et al. [7] show a method for the fast estimation of a battery by using a calorimetric method based on the inversion of a thermal model. The fast estimation of a nearly continuous curve of entropy-variation is proposed.

The mentioned methods are related to determining the entropy change, which has difficulty if given precision as the priority. Therefore, this work represents a new experimental method, which is simple and can precisely estimate the heat generation by maintaining the difference between the battery cell temperature and the ambient temperature to be close to zero as much as possible.

2. THEORY

2.1 Heat Source Terms for the Battery

Heat is always generated within the battery pack during both charging and discharging process. The most common equation used to calculate the heat generation in a cell battery during the charge and discharge cycles is given by:

$$Q_{Battery} = Q_{Overpotential} + Q_{Entropic} \quad (1)$$

2.1.1 Overpotential heat

Overpotential heat is caused by the current flow through the internal resistance in the battery cell. It can be expressed in equation 2.

$$Q_{Overpotential} = I^2 \cdot R_{\eta} \quad (2)$$

2.1.2 Entropic heat

Entropic heat is the heat from the entropy change during the chemical reaction. It can be expressed in equation 3.

$$Q_{Entropic} = -T \bullet \Delta S \bullet \frac{I}{n \bullet F} \quad (3)$$

From the first law of thermodynamics, also known as the conservation of energy principle, states that *"*energy can neither be created nor destroyed during a process; it only change a forms*"* [8].

To determine energy balance, the net change of energy in the system during a process is the difference between the total energy entering the system and the total energy leaving the system, as shown in equation 4.

$$E_{in} - E_{out} = \Delta E_{system} \quad (4)$$

Energy of the system does not change as long as the system state remains static. This value does not change if the system state does not change. In this experiment, ΔE_{system} is determined to be zero since the system does not change its state during the process. Consequently, energy balance of this system can be express in equation 5.

$$Q_{Battery} - Q_{Conduction} - Q_{Convection} - Q_{Radiation} - Q_{Sensible} - Q_{Latent} = 0 \quad (5)$$

In the testing, the battery cell is tested under 4 different situations as depicted in Fig. 1. The descriptions are as following.

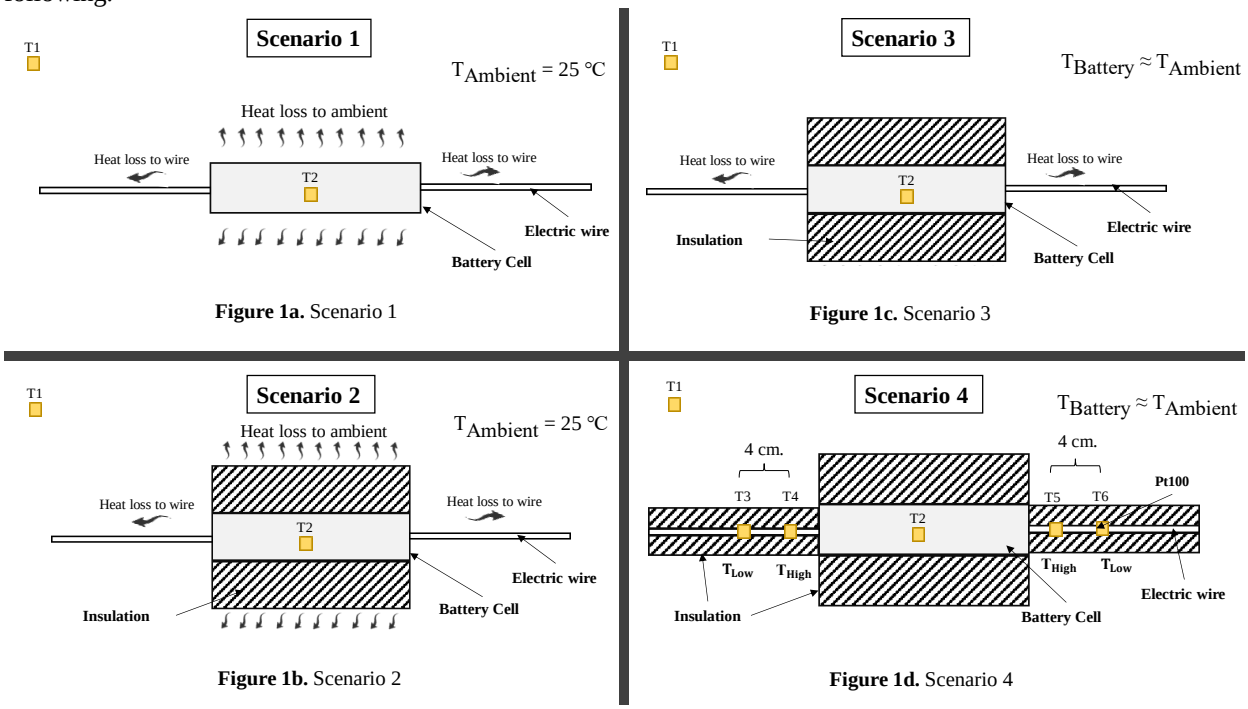

Figure 1a. Scenario 1

Figure 1c. Scenario 3

Figure 1b. Scenario 2

Figure 1d. Scenario 4

Fig. 1. Schematic of the testing scenarios is used in this work

First Scenario: The battery cell is tested at the room temperature without insulation. The heat conduction, heat convection, heat radiation and sensible heat are generated. Latent heat can be neglected due to no phase change in the system. The heat conduction, heat convection, heat radiation cannot be determined in this scenario because it needs high technique for finding. Therefore, the 1st Scenario is not considered. It can be expressed in equation 6.

$$Q_{Battery} - Q_{Conduction} - Q_{Convection} - Q_{Radiation} - Q_{Sensible} - Q_{Latent} = 0 \quad (6)$$

Second Scenario: The heat loss to ambient is reduced by covering an insulator around the battery cell; therefore, the heat convection and heat radiation are nearly zero. In addition, there is not latent heat because of no phase change. Consequently, the equation 5 can be derived as shown in equation 7.

$$Q_{Battery} - Q_{Conduction} - Q_{Convection} - Q_{Radiation} - Q_{Sensible} - Q_{Latent} = 0$$

($Q_{Convection} \approx 0$, $Q_{Radiation} \approx 0$, $Q_{Latent} \approx 0$)

$$Q_{Battery} = Q_{Heat\ loss\ to\ ambient} + Q_{Heat\ loss\ to\ wire} + Q_{Sensible} \quad (7)$$

However, some heat losses occur in term of heat conduction to the insulation and the electric copper wire does not measure. Thereby, equation 7 only remains the sensible heat term that can be expressed in equation 8.

$$Q_{Battery} = Q_{Sensible} = m \cdot C_p \cdot \Delta T \quad (8)$$

Third Scenario: The heat loss due to heat conduction via the insulator is eliminated by controlling the difference between the ambient temperature and the battery cell temperature to be close to zero as much as possible. Therefore, the equation 7 can be revised as shown in equation 9. The heat loss to the electric copper wire and the sensible heat terms are substituted in equation 9 as shown in equation 10.

$$Q_{Battery} = Q_{Heat\ loss\ to\ wire} + Q_{Sensible} \quad (9)$$

$$Q_{Battery} = Q_{Sensible} = m \cdot C_p \cdot \Delta T \quad (10)$$

***Forth Situation**:* Almost heat losses are considered by eliminating the heat loss to ambient and concerning about heat loss to the electric wire of both sides which are used for charging/discharging ports. Two temperature sensors, the distance of which is 4 cm, are attached at each side of the electric wires to measure the temperature difference for calculating the heat loss via the electric wire. In consequence, the heat loss to wire term in equation 9 can be revised to equation 11.

$$Q_{Battery} = \frac{kA}{L} \cdot \Delta T + m \cdot C_p \cdot \Delta T \quad (11)$$

3. EXPERIMENTAL SETUP

3.1 Characterization of battery cell

The cells tested in this study are commercial 18650 lithium-ion cells from Toriyama and Panasonic with NMC (Li-Ni-Mn-Co) and NCA (Li-Ni-Co-Al) as cathodes, respectively. The cells are selected as they have different capacities. The specifications of the cells are listed in Table 1. The two samples in the experiment are referred to as Sample 1 for Toriyama brand and Sample 2 for Panasonic brand in this paper.

Table 1: Specifications of the Li-ion battery cells used.

	TORIYAMA-N18650CL-29	PANASONIC-NCR18650GA
Cell dimension	Height: 64.85± 0.25 mm Diameter: 18.35± 0.15 mm	Height: 65.30 mm Diameter: 18.50 mm
Mass	46.137 g	47.043 g
Cell Type	NMC	NCA
Nominal voltage	3.6 V	3.6 V
Cut-off voltage	2.50 V	2.50 V
Capacity	2750 mAh	3300 mAh

3.2. Experimental setup

To perform the experiment, the battery cells are attached to a battery analyzer machine. This machine can perform different charge and discharge profiles on the cell while monitoring its voltage and current with the BA400WIN software program.

In order to measure the total heat generation of the battery cell during charging and discharging process, the inside wall of the heating chamber is covered with thermal insulation. The major contents of the experimental setup for the 1st, the 2nd, the 3rd, and the 4th scenario include:

(1) For the 1st scenario, this scenario is tested at the room temperature (25 ℃). The battery cell does not cover with insulation. It can express in the Fig. 1a.

(2) For the 2nd scenario, the battery cell is tested at the room temperature (25 ℃). The battery cell is covered with insulation. As shown in Fig. 1b.

(3) For the 3rd scenario, the battery cell is performed the same as the 2nd situation, but the difference between the ambient temperature and the battery cell temperature to be close to zero as much as possible. As shown in Fig. 1c.

(4) For the 4th scenario, there are six temperature sensors (PT100) which are attached inside the test area of the heating chamber as shown in Figure 1d. T1 reads the room temperature, T2 reads the temperature at the surface of the battery cell. T3-T6 read the temperatures of the electric wires at the position shown in the Fig. 1d. It is assumed the cell battery is the lumped model; consequently, the temperatures of the cell are the same at every points. The distance

between the temperature sensors in each wire which are T3- T4 and T5- T6 are set at 4 cm because this is an appropriate distance due to simulation via finite element software. The sensors cannot differentiate temperature variations with the distances of less than 4 cm. The larger distances result in more heat losses to the ambient. Furthermore, the temperature in the heating chamber is maintained at the level of the difference between the battery cell temperature and the ambient temperature (approximately 0.5℃ in this experiment) for the reduction of the heat transfer between the system and the environment.

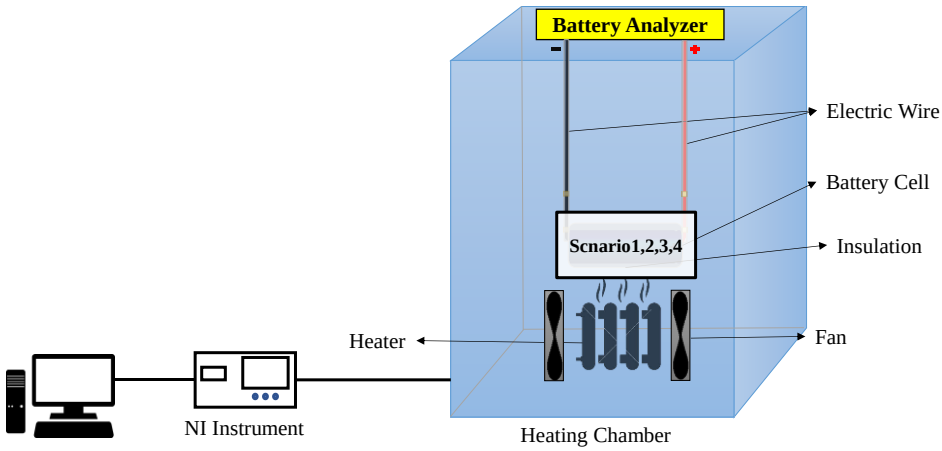

Fig. 2. Schematic of the heating chamber used in this work

Figure 2 shows a schematic diagram of the heating chamber is used in this work. The cell is hung in the air. The battery cell and electric wire are set as the scenario as mention above. The fans are attached to the left and right of the heater for circulating the temperature in the chamber. The heater is controlled via LabVIEW™. The battery analyzer is controlled by the BA400WIN software program and data is logged at a sampling time of 0.5 seconds to the computer.

3.3. Testing heat generation of battery cells

The battery cells are tested as an individual cell at different constant C-rates. Each sample is tested its charging cycle at different C-rate because of the maximum charge current is limited. Sample 1 is tested at 0.25C, 0.5C, and 0.75C while Sample 2 is tested at 0.25C, 0.5C, and 0.65C. For discharging cycles, the battery analyzer machine is limited current at 3 A. therefore, the discharge is tested only at 1C. The heat generation is monitored in the range of the State of Charge (SOC) of the cell. In the testing, the battery cell is tested under 4 different situations as depicted in Fig. 1. The descriptions are as following.

1st Scenario: The cell is tested at the room temperature without insulation. The heat conduction, heat convection, heat radiation and sensible heat are generated. Latent heat can be neglected due to no phase change in the system. The heat conduction, heat convection, heat radiation cannot be determined in this scenario because it needs high technique for finding. Therefore, the 1st Scenario is not considered.

2nd Scenario: The cell is tested at the room temperature with insulation. The heat radiation and latent heat can be neglected because the battery cell is covered with insulation and there is no phase change. However, some heat losses occur in term of heat conduction to the insulation and the electric copper wire.

3rd Scenario: The cell is tested under the adiabatic environment with insulation. The difference of the temperature between the ambient and the battery is maintained to be close to zero as much as possible. The heat convection, heat radiation, and latent heat can be neglected. There is some heat loss to the electric copper wire. In this situation, heat conduction to the electric copper wire is not measured.

4th Scenario: The cell is tested under the adiabatic environment and the heat loss in the electric wire is measured. The heat convection heat, heat radiation and latent heat can be neglected. Therefore, the heat conduction and sensible heat are calculated. In this case, heat conduction to the electric copper wirecan be calculated by using PT100 attaches on the electric wire for measuring the variation of temperature at low and high points.

3.4. Heat calculations

In order to calculate of the heat generation during charge – discharge based on the energy balance model, equation 4 is used. The specific heat capacity (C_p) of the battery are required, which can be approximated to be 842 J/kg °C for Sample 1 and 1,037.4 J/kg °C for Sample 2 based on the published value [9-16]. Other parameters involved in the equation such as the thermal conductivity (k) of copper [16], the surface area (A) for the heat transfer in the electric wire is 0.000000823 m^2 because AWG 18 is used, the distance between temperature sensors (L) in electric wire is 0.04 m. as shown in Table 2.

Table 2: Model Parameter

Parameter	**Unit**	**Value**	
Specific heat capacity (C_p)	J/kg °C	Sample 1	Sample 2
		842	1,037.4
Thermal conductivity (k)	W/m°C	395	
The surface area (A)	m^2	0.000000823	
Distance between Sensor (L)	m	0.04	

4. RESULTS

4.1. Comparison of Heat generation in each scenario on battery cell

In order to explore the thermal characteristic of battery cell during charging process, the battery cell is tested at the constant current (CC) and the constant voltage (CV) modes. The results in Fig. 3 show that the current remains constant at the beginning of the charging process under CC mode, and then, the current sharply drops at approximately 90 % of SOC as the battery is nearly fully-charged.

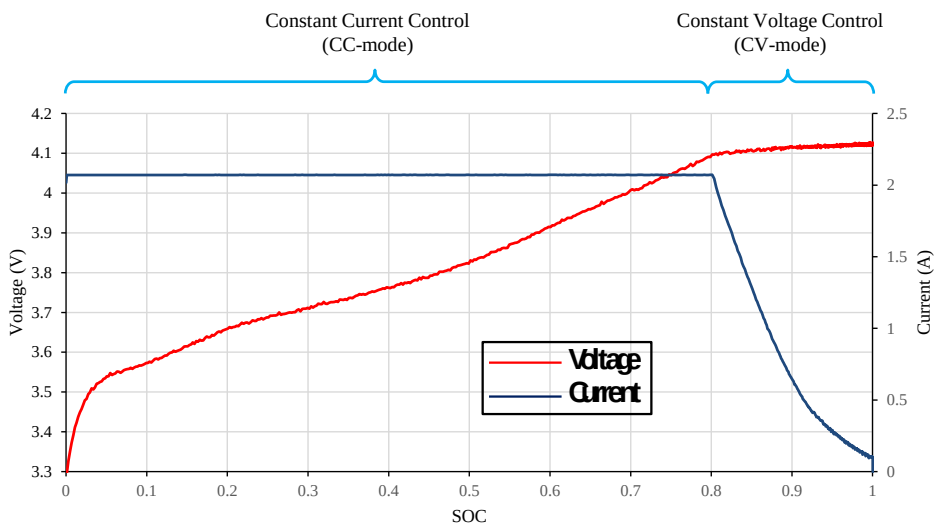

Fig. 3. Constant Current Control (CC Mode) and Constant Voltage Control (CV Mode) of the sample 1 at charging 0.75C

In this work, the method to measure and calculate heat generation of the battery cell has been explained in the section 3. The result in this paper shows the comparison of the charging process at 0.75C between 4 different situations on Sample 1. Heat generation is plotted in Fig. 4.

1st scenario*:* The heat generation of battery cannot be calculated due to the variation of the temperature at the cell surface has a little change. Therefore, it cannot be determined.

2nd scenario*:* Heat generation of the battery cell is little because there is heat loss due to the conduction via the insulation and the electric wire.

3rd scenario: Heat generation of the battery cell can be calculated by using the formula of sensible heat but there is some heat loss to the copper conductor.

4th scenario: heat generation of the battery cell can be calculated by using equation 11.

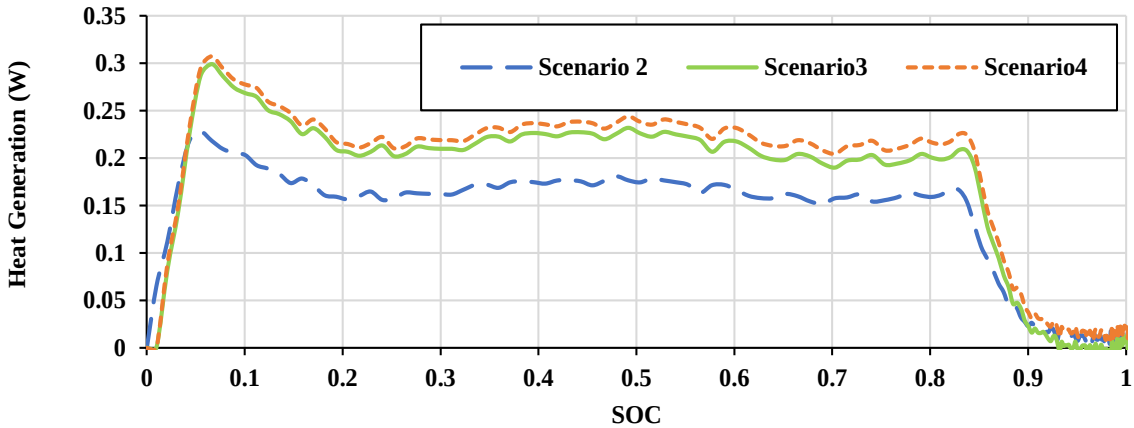

Fig. 4. Comparison of heat generation in charging process at 0.75C on Sample 1

This experimental data of the charging cycle as shown in Fig. 4. The maximum heat value of 2nd scenario, 3rd scenario and 4th scenario are 0.228 W, 0.299 W, and 0.307 W, respectively. The 2rd scenario is a normal method for finding the heat generation in a battery cell. If the 2rd scenario is set the heat generation as a reference value. The 3nd scenario can be measured the heat generation more than the 2rd scenario is approximately 31.140 percent. While the 4th scenario is found to be the heat generation in a battery cell is more than the 2rd scenario is approximately 34.649 percent. The comparison between three scenarios, the 4th scenario is precisely method for measure the heat generation. Besides, the surface temperature of battery cell gradually increased from 0 to 0.9 of SOC, and then it remains steady due to the less heat generated at the end of charging process. This phenomenon can be supported by the current as shown Fig. 3.

4.2. Comparison of Heat generation in each type of battery cell

In this work, the method to calculate heat generation of the battery cell has been explained in the section 2. Heat generation of the Sample 1 and Sample 2 are plotted in Fig. 5, 6, 7, and 8. This experimental data of the charging cycle will be plotted to compare the different current rates of the cells in order to further provide the proper cooling system. While the discharging cycle showing the current at 1C is repeated three times. During the cycle, the maximum heat generation of Sample 1 is less than Sample 2 due to their specific heat capacities. Since Sample 2 has a capacity more than Sample 1.

The generated heat during the charging condition at the beginning period had risen sharply and then decreased sharply again at the end of the charge process because the current flow through the battery are decreasing [17] as shown in Fig. 3. On the other hand, heat at the discharge process sharply increased at the beginning period because of high resistance of the cell. At the end of the discharge process, the generated heat quickly decreases as shown in Fig. 7 and 8. From the Fig. 5 and 6, when C-rate increases, the heat generation of a battery also increases according to equation 1. All this experimental result is tested under 4th Situation.

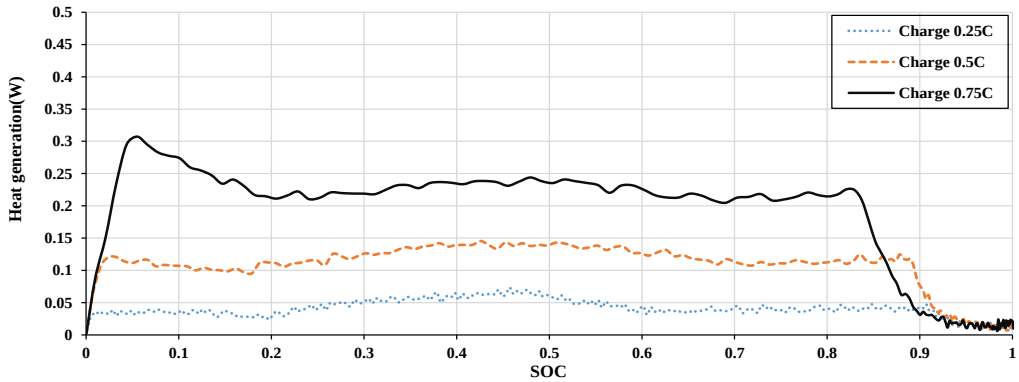

Fig. 5. Comparison on the heat generation at different C-rate during charge of Sample 1

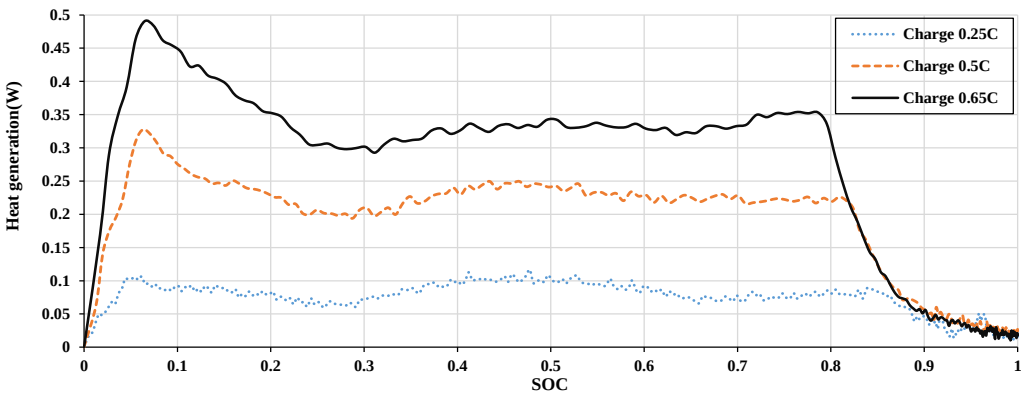

Fig. 6. Comparison on the heat generation at different C-rate during charge of Sample 2

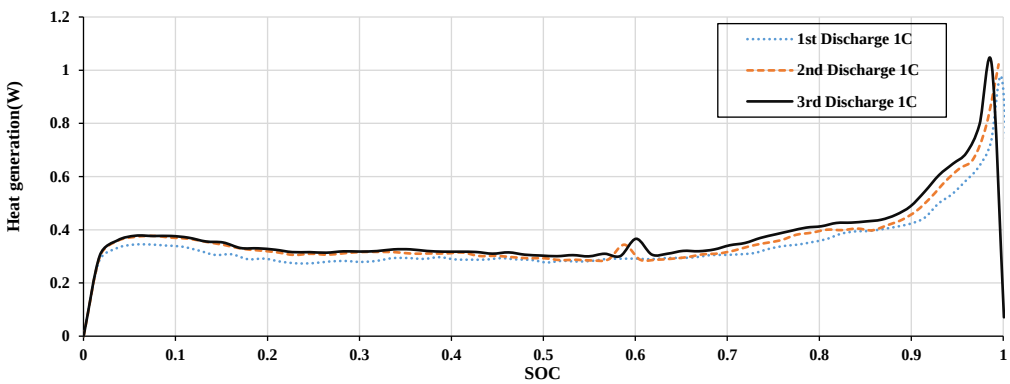

Fig. 7. The heat generation at 1C-rate during discharge of Sample 1

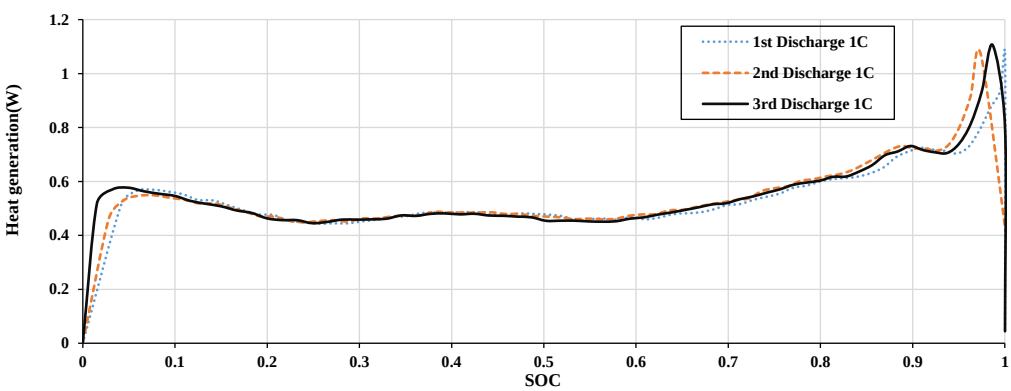

Fig. 8. The heat generation at 1C-rate during discharge of Sample2

The variations of the maximum heat generation, the heat loss, and the maximum temperature at the surface are found experimentally i.e. from 100% SoC to 0% SoC or 0% SoC to 100% SoC are tabulated in Table 3.

Table 3: Summary of the result

Type of Samples	Event	Charge			Discharge		
Sample 1	Current Rate	0.25C	0.5C	0.75C	1st1C	2nd1C	3rd1C
	Max Heat Generation (W)	0.073	0.145	0.3070	0.953	1.022	1.041
	Maximum Temperature (°C)	36.361	41.709	45.813	51.813	52.462	53.012
Sample 2	Current Rate	0.25C	0.5C	0.65C	1 st1C	2 nd1C	3rd1C
	Max Heat Generation (W)	0.117	0.323	0.491	1.076	1.0959	1.2405
	Maximum Temperature (°C)	43.773	50.812	53.964	61.839	62.667	63.187

5. CONCLUSION

There are numerous methods to measure the heat generation of the Li-Ion battery cell. The aimed of this article is to find the new method for heat calculation of the battery cell. The battery cell is tested under the four situations at the different charge/ discharge rate. The results found that the testing under the adiabatic environment and the measurement of the heat loss from the electric wire (4^{th} Scenario) is found to be the best method comparing with another situations because its can measure the heat generation more than 2^{nd} scenario approximately 35 percent. In addition, the amount of heat generated by the battery cell is associated with the corresponding current. Consequently, this method can be obtained precisely estimation heat generation in a battery cell. The precise heat generation of battery cell can promote the designing of a battery thermal management system (BTMS) for the safety of lithium batteries.

NOMENCLATURE

$Q_{Battery}$	total heat generation in the battery cell, W
$Q_{Overpotential}$	heat generated in term of Joule heating, W
$Q_{Entropic}$	heat generated due to Entropy change, W
I	applied current, A
R_η	overpotential resistance, Ω
T	temperature of the cell, K
ΔS	entropy change, J/K
n	number of electrons, mole
F	Faraday's constant, ($9.648456 \cdot 10^4$ C/mole)
$Q_{Conduction}$	heat lost due to heat conducted into the electric wire of battery cell, W
$Q_{Convection}$	heat lost to convective heat transfer to the air around at surface of battery cell, W
$Q_{Radiation}$	heat lost by energy emitted in form of electromagnetic waves through air particle, W
$Q_{Sensible}$	internal heat of the battery with measured capacity and temperature, W
Q_{Latent}	internal energy associated with the phase change of the system, W
k	thermal Conductivity, W/m°C
L	length of wire, m
A	surface area of material, m^2
ΔT	temperature gradient, °C
m	mass of battery cell, kg
C_p	specific heat capacity, J/kg°C

Acknowledgments

The authors are support given by National Energy Technology Center (ENTEC) is a member of the National Science and Technology Development Agency **(**NSTDA**)** and Thailand Advanced Institute of Science and Technology-Tokyo Institute of Technology **(**TAIST-Tokyo Tech**)** for financial support.

References

[1] Xu, B., Oudalov, A., Ulbig, A., Andersson, G., Kirschen, D.S. Modeling of lithium-ion battery degradation for cell life assessment, IEEE Transactions on Smart Grid, Vol. 9(2), 2018, pp. 1131-1140.

[2] Abdul-Quadir Yasir, M.P.K., Laurila, T., Karppinen, J., Jalkanen, K., Vuorilehto, K., Skogström, L. Heat generation in high power prismatic Li-ion battery cell with LiMnNiCoO2 cathode material, International Journal of Energy Research, Vol. 38(11), 2014, pp. 1424-1437.

[3] Bai, Y., Li, L., Li, Y., Chen, G., Zhao, H., Wang, Z., et al. Reversible and irreversible heat generation of NCA/Si-C pouch cell during electrochemical energy-storage process, Journal of Energy Chemistry, Vol. 29, 2019, pp. 95-102.

[4] Wang, Z., Tong, X., Liu, K., Shu, C.M., Jiang, F., Luo, Q., et al. Calculation methods of heat produced by a lithium-ion battery under charging-discharging condition, Fire and Materials, Vol. 43(2), 2018, pp. 219-226.

[5] Lin, C., Wang, F., Fan, B., Ren, S., Zhang, Y., Han, L., et al. Comparative study on the heat generation behavior of lithium-ion batteries with different cathode materials using accelerating rate calorimetry, Energy Procedia, Vol. 142, 2017, pp. 3369-3374.

[6] Chanthevee, P., Hirai, S., Lailuck, V., Laoonual, Y., Sriam, P., Rompho, S., et al. A simplified approach for heat generation due to entropy change in cylindrical LCO battery, paper presented in 2018 IEEE Transportation Electrification Conference and Expo, Asia-Pacific, 2018, IEEE, Bangkok.

[7] Damay, N., Forgez, C., Bichat, M.P., Friedrich, G. A method for the fast estimation of a battery entropy-variation high-resolution curve – Application on a commercial LiFePO4/graphite cell, Journal of Power Sources, Vol. 332, 2016, pp. 149-153.

[8] Cengel, Y. and Ghajar, A. Heat and mass transfer: Fundamentals and applications, 5th edition, 2015, McGraw-Hill Education, New York.

[9] Bubbico, R., D'Annibale, F., Mazzarotta, B., Menale, C. Thermal model of cylindrical lithium-ion batteries, Chemical Engineering Transactions, Vol. 74, 2019, pp. 1291-1296.

[10] Jeon, D.H. and Baek, S.M. Thermal modeling of cylindrical lithium ion battery during discharge cycle, Energy Conversion and Management, Vol. 52(8-9), 2011, pp. 2973-2981.

[11] Zheng, G., Zhang, W., Huang, X. Lithium-Ion battery electrochemical-thermal model using various materials as cathode material: A simulation study, ChemistrySelect, Vol. 3(41), 2018, pp. 11573-11578.

[12] Morganti, M.V., Longo, S., Tirovic, M., Blaise, C.Y., Forostovsky, G. Multi-Scale, Electro-Thermal model of NMC battery cell, IEEE Transactions on Vehicular Technology, Vol. 68(11), 2019, pp. 11367-11704.

[13] Lei, B., Zhao, W., Ziebert, C., Uhlmann, N., Rohde, M., Seifert, H. J. Experimental analysis of thermal runaway in 18650 cylindrical Li-Ion cells using an accelerating rate calorimeter, Batteries, Vol. 3(2), 2017, pp. 1-14.

[14] Dong, T., Wang, Y., Peng, P., Jiang, F. Electrical-thermal behaviors of a cylindrical graphite-NCA Li-ion battery responding to external short circuit operation, International Journal of Energy Research, Vol. 43(4), 2019, pp. 1444-1459.

[15] Brodsky, P. Real-time Modeling of battery pack temperature for thermal limit prevention in electric race vehicles, 2016, The Ohio State University, USA.

[16] Königseder, A. Investigation of the thermal runaway in lithium ion batteries, 2017, Graz University of Technology, Austria .

[17] Haniff Mahmud, A., Hilmi Che Daud, Z., Asus, Z. The impact of battery operating temperature and state of charge on the lithium-ion battery internal resistance, Jurnal Mekanikal, Vol. 40, 2017, pp. 1-8.